Case Report

Cerebral oximetry-guided pulmonary artery banding for end-stage heart failure in a child with left ventricular noncompaction cardiomyopathy: a case report

Mayu Asano^, Kenji Doi, Minoru Nomura, Yasuko Nagasaka

Department of Anesthesia, Tokyo Women's Medical University, Tokyo, Japan

Correspondence to: Kenji Doi, MD. Department of Anesthesia, Tokyo Women's Medical University, 8-1 Kawadacho, Shinjukuku, Tokyo 162-8666, Japan. Email: doi.kenji@twmu.ac.jp.

Abstract: Pulmonary artery banding (PAB) may reduce the need for left ventricular assist devices and heart transplantation in children with end-stage heart failure. However, excessive banding may increase the right ventricular afterload, leading to worsening of heart failure. The estimated right ventricular pressure and the shifting of the interventricular septum by transesophageal echocardiography (TEE), pulmonary artery pressure, right atrial and ventricular pressure, percutaneous oxygen saturation, and mixed venous oxygen saturation are utilized to determine the optimal circumference for PAB. Here, we report the case of a 5-month-old patient with end-stage heart failure due to left ventricular noncompaction cardiomyopathy (LVNC), with a gene mutation of MYH7, who underwent successful PAB. The exact PAB placement was additionally guided by using cerebral regional oxygen saturation (rSO_2) measurement to achieve a tolerable and optimal PAB effect. We monitored rSO_2 and other hemodynamic parameters while surgeons banded the pulmonary artery to achieve both highest rSO_2 levels and stable hemodynamics. rSO_2 was 68% before banding, and increased and remained at over 90% after the banding at same FiO_2. Patient's heart failure improved gradually, and the child was discharged home at 6 months after PAB. The rSO_2 is a simple and non-invasive monitor for the measurement of oxygen delivery to the brain tissue. rSO_2 alone would not be able to guide PAB placement in the vulnerable DCM patients, but it may be of one further monitoring value for the optimal pulmonary artery circumference while patients are undergoing PAB.

Keywords: Case report; cerebral oxygen delivery; left ventricular noncompaction (LVNC); pulmonary artery banding (PAB); regional oxygen saturation (rSO_2)

Submitted Jul 22, 2021. Accepted for publication Oct 21, 2021.
doi: 10.21037/tp-21-340
View this article at: https://dx.doi.org/10.21037/tp-21-340

Introduction

Left ventricular noncompaction cardiomyopathy (LVNC) is caused by the impaired development of compactional myocardial structures in the fetal period, resulting in the development of cardiomyopathy of the left ventricle. An enlarged left ventricle may present with a dilated cardiomyopathy (DCM)-like pathology. Inadequate contraction restricts cardiac output, leading to a poor prognosis and ultimately the need for heart transplantation. Pulmonary artery banding (PAB) as medical treatment for end-stage heart failure in DCM, including LVNC, may help in controlling the progression of symptoms as well as improve prognosis (1,2). However, there is no universal measures to obtain optimal PAB, thus, procedural approaches must be individualized.

Measurement of regional oxygen saturation (rSO_2),

^ ORCID: 0000-0001-9771-6002.

which represents systemic oxygen delivery by near-infrared spectroscopy, serves as alternative monitoring method for mixed venous oxygen saturation (SvO_2) (3). Therefore, we utilized rSO_2 monitoring to ensure adequate cerebral oxygenation while adjusting the pulmonary artery circumference for PAB, in a pediatric patient with LVNC.

We present the following case in accordance with the CARE reporting checklist (available at https://dx.doi.org/10.21037/tp-21-340).

Case presentation

A 5-month-old male patient, born at 40 weeks and 3 days by vaginal delivery (birth weight, 3,562 g), had an Apgar score of 8 and 9 at 1 and 5 minutes, respectively. He was noted to have cardiomyopathy at the fetal stage (25 weeks of gestation). Postnatal transthoracic echocardiography (TTE) confirmed LVNC by non-compacted layer and the atrial duct was still patent with the presence of an atrial communication. Subsequently, a diagnosis of LVNC was made. The genetic testing of the patient revealed a MYH7 heterozygous missense variant (NM_000257.3: c. 1180G>A: pAsp394Asn.), however, his parents were not tested for genetic mutations. He was intubated on the day of birth because of decreased left ventricular contraction and was started on β-blocker, angiotensin converting enzyme inhibitor, diuretics (furosemide, spironolactone, tolvaptan), dobutamine, and olprinone infusion. Patent ductus arteriosus ligation was performed on postnatal day 8 in previous hospital.

Due to the worsening of his heart failure, he was transferred to our hospital while still intubated at postnatal 12 weeks. Upon arrival to our hospital, his vital signs were notable for, noninvasive blood pressure (NBP) of 75/46 mmHg, heart rate (HR) of 120/min, and saturation of percutaneous oxygen (SpO_2) of 98% at a fraction of inspiratory oxygen (FiO_2) of 0.6. His brain natriuretic peptide (BNP) level was 954 pg/mL. He was on dobutamine (4 mcg/kg/min) and olprinone (0.3 mcg/kg/min).

Although he was extubated at postnatal 15 weeks, his nutritional status remained poor, and his urine output was scarce. TTE at 19 weeks showed left ventricular ejection fraction (LVEF) of 28.8%, left ventricular internal dimension diastole (LVIDd) of 3.0 cm (z-score 5.6, normal range, 1.1–2.4), mild tricuspid valve regurgitation (TR, maximum velocity was 2.5 m/sec), estimated right ventricular pressure was 35 mmHg, mild mitral regurgitation (MR), and 1.5 mm atrial septal defect (ASD). Noncompaction area in the LV apex to apical lateral, and LVEF of the area was reduced. The non-compacted layer to compacted layer in a ratio of more than 2:1 (*Figure 1A-1C*). His chest X-ray was notable for cardiomegaly with pulmonary congestion (*Figure 2*). Magnetic resonance imaging (MRI) at 21 weeks showed a left ventricular end diastolic volume (LVEDV) of 19.3 mL (=96.5 mL/m^2, z-score 6.72, normal range 8.2–12.1), right ventricular end diastolic volume (RVEDV) of 13 mL (=65 mL/m^2, z-score 2.8, normal range 7.6–11.9), and LVEF of 33%, and right ventricular ejection fraction (RVEF) of 47.7% (*Figure 3A,3B*). These results were consistent with bi-ventricular enlargement and low ejection fraction. Because the medical treatment for his heart failure was only limited, after a multidisciplinary meeting, the patient was scheduled for PAB to control the progression of heart failure (1). His surgery was also planned as a bridge therapy to the left ventricular assist device implantation and heart transplantation in the future, given the extreme shortage of pediatric heart donors available in Japan. At postnatal 22 weeks, the decision of surgery for PAB was made. Preoperative blood test results were normal, he was on trans-gastric medications (furosemide 6 mg/day, spironolactone 3 mg/day, tolvaptan 0.92 mg/day, carvedilol 1.1 mg/day, enalapril maleate 0.2 mg/day), and intravascular medications (dobutamine 3 mcg/kg/min and a maximum dosage of olprinone at 0.3 mcg/kg/min). Olprinone is one of the phosphodiesterase-3-inhibitors, given for patients with acute heart failure, at the maintenance dose of 0.1–0.3 mcg/kg/min after an initial bolus period.

On the day of surgery, his body weight was 3.2 kg. Systolic and diastolic blood pressures were 109/66 mmHg, heart rate was 135/min, SpO_2 was 100% and rSO_2 was 54% after the induction of anesthesia. Anesthesia was induced using midazolam and fentanyl. Thereafter, rocuronium was administered and the patient was intubated and mechanically ventilated. Midazolam, fentanyl, and remifentanil were administered for the maintenance of anesthesia. Preoperative dobutamine (3 mcg/kg/min) were continued, adrenaline was initiated, and preoperative olprinone (0.3 mcg/kg/min) was changed to milrinone (0.5 mcg/kg/min) due to the concerns for vasodilatory effects of olprinone, vs. milrinone after the cessation of cardiopulmonary bypass (4). A peripheral venous line, radial arterial line, and central venous catheter were inserted. Initial central venous pressure (CVP) was 1 mmHg. To monitor real-time changes in rSO_2, an anterior forehead rSO_2 monitor (INVOS™ 5100, Covidien

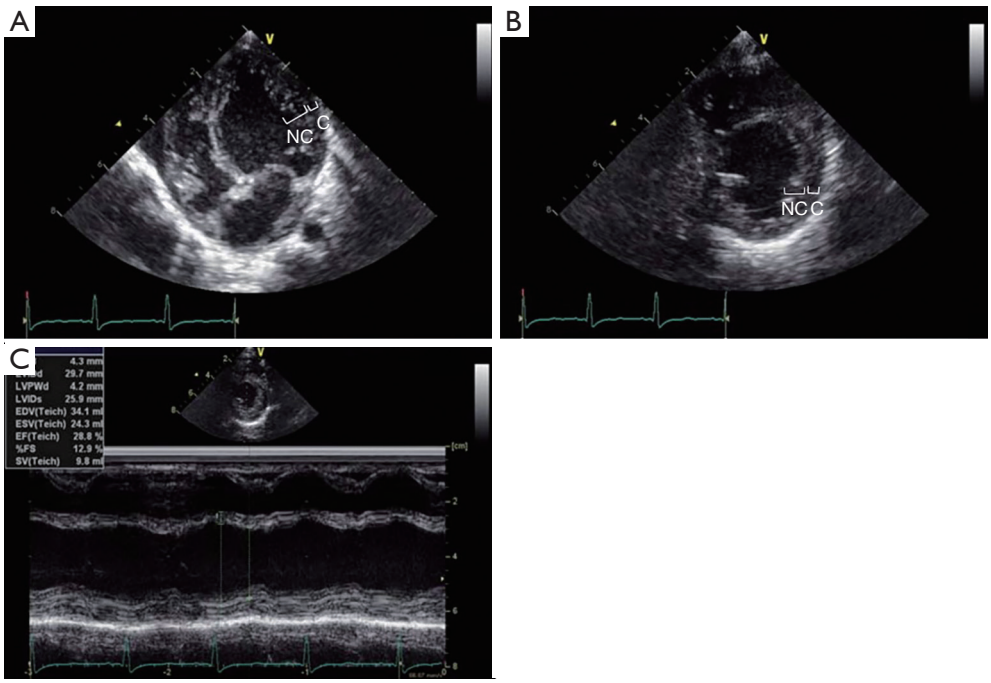

Figure 1 Transthoracic echocardiography before the PAB. (A) Transthoracic four-chamber view demonstrated LV non-compaction, indicated by the non-compacted myocardial layer to compacted layer in a ratio of more than 2:1, most prominent in the apical to the lateral region of the LV. (B) Reduced LV systolic function was notable for the LV non-compacted area on the LV short-axis view. (C) Reduced LV contraction, LVEF 28.8% by the Teichholz formula (%FS of 12.9), were noted by the M-mode measurement of the LV. PAB, pulmonary artery banding; LV, left ventricle; LVEF, left ventricular ejection fraction; NC, non-compacted layer; C, compacted layer.

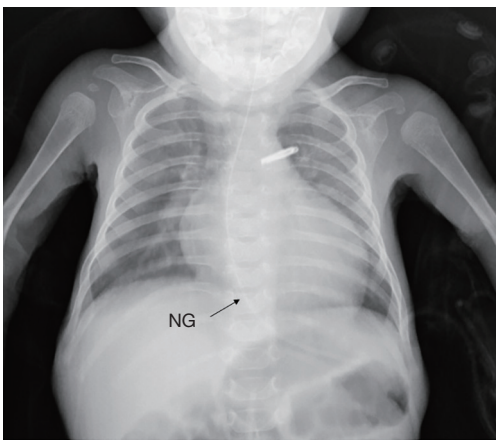

Figure 2 Chest X-Ray images before the PAB. Chest X-ray images, both before and after the PAB, show pulmonary congestion and cardiomegaly. CTR 57.1%. PAB, pulmonary artery banding; TR, cardio thoracic ratio; NG, nasogastric tube.

Japan, Co., Tokyo, Japan) was applied. rSO_2 shows the tissue oxygen saturation of the microcirculation 2–3 cm below the sensor and the oxygen hemoglobin of the arteriovenous mixture. Therefore, rSO_2 reflects changes in arterial blood oxygen saturation, cardiac output, hemoglobin concentration. One can place an adhesive sensor to the anterior forehead to measure the tissue oxygen saturation level, and thus the increase or decrease of oxygen supply to the cerebrum. It is important to monitor the changes in rSO_2, as it is often impacted by changes in hemodynamics because rSO_2 is a relative value, not an absolute value. Transesophageal echocardiography (TEE) under general anesthesia was performed to monitor cardiac function during surgery, shitting of the interventricular septum, and exacerbation of the severity of valvular regurgitation throughout the procedure. The pre-operative TEE revealed non-compacted myocardial layers inferior to the lateral walls, mild TR (maximum velocity of 2.7 m/sec), estimated right ventricular

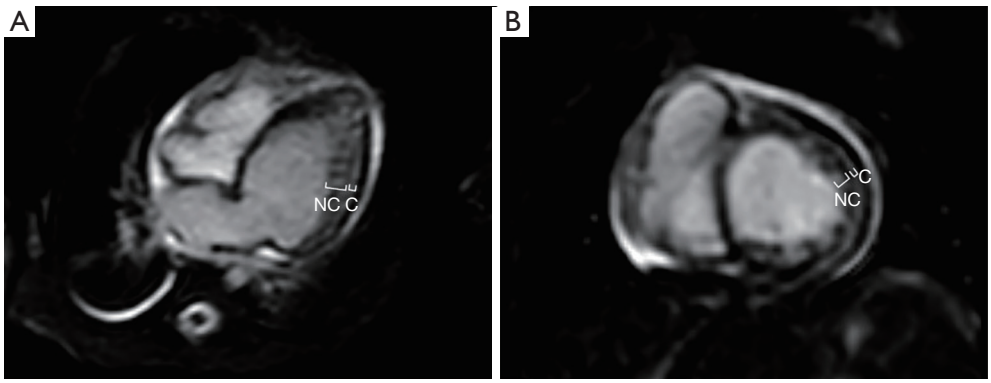

Figure 3 Magnetic resonance imaging before PAB. The non-compacted layer was 9 mm and the compacted layer was 3 mm, indicating the NC to C ratio >2:1. (A) 4-chamber view. (B) Short axis view. NC, non-compacted layer; C, compacted layer.

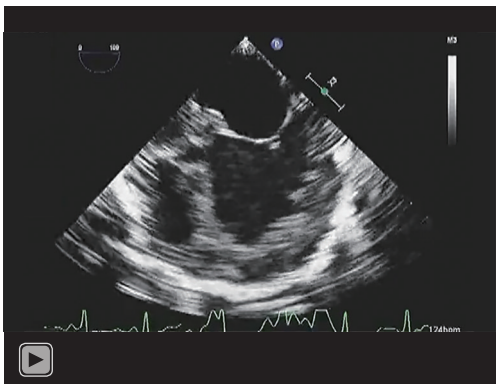

Video 1 Intraoperative TEE before the PAB. Dilated LV, with prominent non-compacted myocardial layer in the inferior and lateral walls were noted. Reduced right ventricular motion was observed. TEE, transesophageal echocardiography; PAB, pulmonary artery banding.

pressure of 31 mmHg, trivial MR, and ASD was found to be closed naturally on the day of surgery (*Video 1*).

After a median sternotomy, a tape, which was cut from the 0.4 mm expanded polytetrafluoroethylene patch, was passed behind the main pulmonary artery. The main pulmonary artery was strangulated with polypropylene suture. The surgeon estimated the circumference to be around 23 mm according to the Trusler's formula (5). He passed the band around the PA, tightening 1 mm at a time to carefully determine the optimal circumference to enable the highest rSO_2 and stable CVP levels. In addition, we determined the optimal circumference by via three main features on the TEE: (I) the velocity across the PAB using continuous-wave Doppler, (II) degree of TR, and (III) visual monitoring of the shift of interventricular septum. Finally, PAB was secured at a mid-pulmonary artery circumference of 23 mm. We continuously monitored rSO_2, vital signs, velocity across the PAB with continuous wave Doppler by TEE until end of the procedure. After banding, SpO_2 decreased from 100% to 98%, and rSO_2 increased from 68% to 91% at an FiO_2 of 0.5 throughout the surgery (*Figure 4*). Intraoperative TEE after the PAB showed mild TR (maximum velocity was 3.0 m/sec), estimated right ventricular pressure of 38 mmHg (derived from the concurrent CVP of 2 mmHg), trivial MR, and the velocity across the PAB with continuous wave Doppler of 2.4 m/sec. We observed shifting of the interventricular septum to the left ventricle, narrowing of the left ventricle and expanded right ventricle, and no change in bi-ventricular function (*Video 2*, *Figure 5*).

The patient was extubated at 6 hours after the arrival in the ICU and was transferred to the general floor on day 4 post-surgery. Postoperative TTE at 4-week was notable for slightly improved LVEF of 36%, LVDd of 3.3 mm (+2.2 SD), mild TR (maximum velocity was 2.9 m/s), estimated right ventricular pressure of 44 mmHg, trivial MR, and the velocity across the PAB with continuous wave Doppler of 2.4 m/s, corresponding to a pressure gradient of 23 mmHg. The BNP levels dramatically decreased to 14.0 pg/mL after 2 months. Postoperative inotropes were reduced; olprinone was withdrawn on the day of surgery. Dobutamine was tapered and withdrawn and milrinone was decreased to 0.32 mcg/kg/min. At 3 months after the surgery, his oral drug included furosemide 10 mg/day, spironolactone 8 mg/day, trichlormethiazide 0.4 mg/day, tolvaptan 1.2 mg/day, carvedilol 1.6 mg/day, enalapril maleate 1.2 mg/day, and

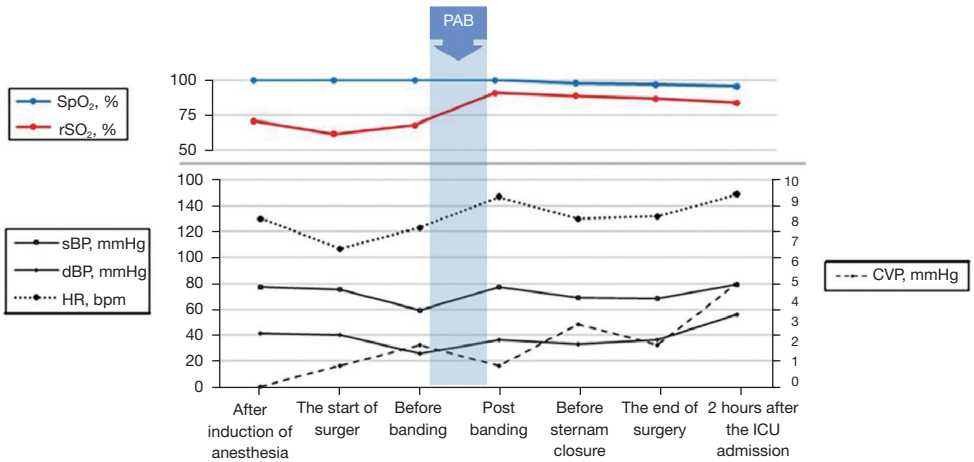

Figure 4 Mean cerebral rSO_2 levels before, during and after the PAB. SpO_2 decreased from 100% to 98%, and rSO_2 increased from 68% to 91% after banding; at an FiO_2 of 0.5. Although a trend in rising the CVP was present, the value was no higher than 5 mmHg at the end of surgery. CVP, central venous pressure; dBP, diastolic blood pressure; FiO_2, fraction of inspired oxygen; PAB, pulmonary artery banding; rSO_2, regional oxygen saturation; sBP, systolic blood pressure; SpO_2, saturation of percutaneous oxygen; HR, heart rate.

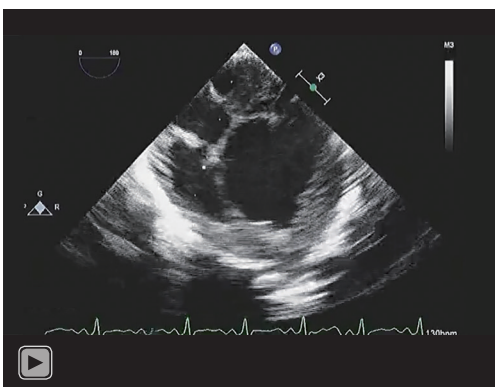

Video 2 Intraoperative TEE after the PAB. Dilated LV, with prominent non-compacted myocardial layer in the inferior and lateral walls were noted. Interventricular septum shifted to the left ventricle, narrowing the left ventricle cavity and dilation of the right ventricle was observed. No change in bi-ventricular systolic and diastolic functions were present. TEE, transesophageal echocardiography; PAB, pulmonary artery banding.

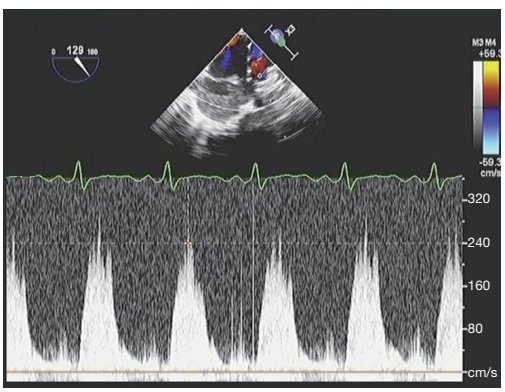

Figure 5 Velocity across the PAB by intraoperative transesophageal echocardiography. During the operation, peak velocity of 2.4 m/sec across the PAB was measured by continuous wave Doppler. PAB, pulmonary artery banding.

aspirin 25 mg/day. TTE performed 3 months after surgery, revealed LVEF of 41%, LVIDd of 3.2 cm (z-score 3.97, normal range 1.5–2.8), mild TR (maximum velocity of 3.0 m/sec), estimated right ventricular pressure of 46 mmHg, trivial MR, and the velocity across the PAB was 3.2 m/sec on continuous wave Doppler (*Figure 6A*,*6B*). There was little change in the X-ray after 3 months (*Figure 7*). MRI showed LVEDV of 31 mL (=101 mL/m^2, z-score 6.39, normal range 13.7–20.1), RVEDV of 29 mL (=97 mL/m^2, z-score 5.06, normal range 13.0–20.3), LVEF was 39%, and RVEF was 45% after 4 months. The patient's nutritional status improved postoperatively. Preoperatively, the patient received enteral nutrition (400 mL/day), but 6 months after surgery, he outgrew tube

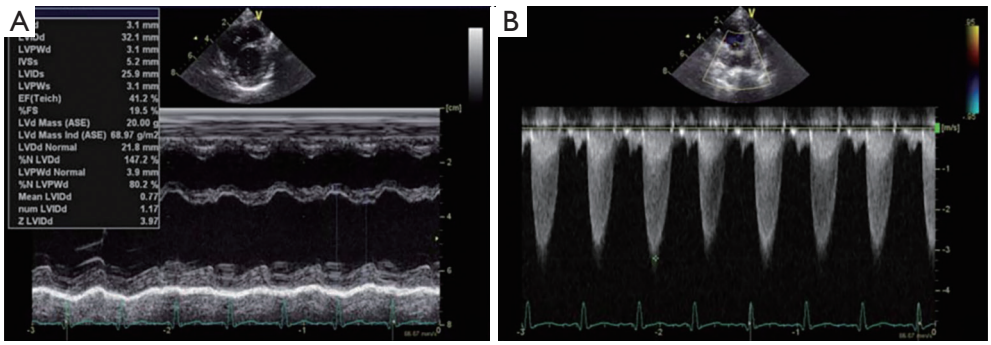

Figure 6 Postoperative transthoracic echocardiography at 3 months after the PAB. Three months after the surgery, left ventricular systolic function was improved to 41% by the Teichholz formula (%FS of 19.5), reduction of LVIDd 3.2 cm was measured. Velocity across the PAB was 3.2 m/sec on continuous wave Doppler. (A) Improvement of LVEF was measured. (B) The velocity across the PAB of 3.2 m/sec on continuous wave Doppler. PAB, pulmonary artery banding; LVIDd, left ventricular internal dimension diastole.

Figure 7 Chest X-ray images after the PAB. Chest X-ray images show pulmonary congestion and cardiomegaly identically before PAB. CTR 57.5%, NG tube was withdrawn. PAB, pulmonary artery banding; CTR, cardio thoracic ratio.

feeding and was able to drink milk and eat three times per day. He was discharged home on the postoperative day 179. His body weight was 6.9 kg at discharge (+3.7 kg/6 months). His discharge medications included furosemide 11 mg/day, spironolactone 11 mg/day, tolvaptan 1.2 mg/day, carvedilol 2.2 mg/day, enalapril maleate 1.8 mg/day, and aspirin 30 mg/day.

All procedures performed in studies involving human participants were in accordance with the ethical standards of the institutional and/or national research committee(s) and with the Helsinki Declaration (as revised in 2013). Written informed consent was obtained from the patient's parent or legal guardian for publication of this case report and accompanying images. A copy of the written consent is available for review by the editorial office of this journal.

Discussion

LVNC is characterized by abnormal trabeculations in the left ventricle, and it can be associated with LVNC-dilatation and systolic or diastolic dysfunction, or both, eventually resulting in DCM-like heart failure (6). The patient had a genetic test that identified a mutation in MYH7. This mutation in MYH7 is associated with DCM and have been reported to account for 3% of DCM patients. This mutation is male-dominated and is characterized by conduction defects in 48% of cases (7).

PAB has been reported as an option for functional regeneration in infants and toddlers with left ventricular DCM with preserved ejection fraction (1). If the heart failure is not controlled with medical intervention, PAB may be applied even in the end-stage LVNC.

PAB in an enlarged left ventricle decreases the left ventricular preload and increases the right ventricular pressure. Previous study suggests that PAB shifts the deviated interventricular septum to the left side, may shift to a near-normal position, if tolerated (8). However, in young infants there is also time to grow-in the PAB, if a tight PAB is not initially tolerated. Reduction of left ventricular end-diastolic volume, diameter and end-diastolic pressure is anticipated, and the improvement of left ventricular function may improve initially, but in particular, over time (8).

PAB reduces pulmonary blood flow in patients with pulmonary over-circulation. Herein, we calculated the

optimal PA circumference using the Trusler's formula (calculated circumference =20 mm +1 mm/kg body weight). However, the optimal circumference for PAB in the patients with heart failure cannot been clearly defined by a simple calculation, as it differs depending on the individual patient's age, condition, myocardial function, and basic hemodynamics. In the clinical settings to palliate patients with ventricular septum defects and pulmonary over-circulation, pulmonary artery pressure and SpO_2 are the two major factors used to determine the PAB circumference (9). However, PAB as a treatment for heart failure is different from the conventional PAB placement and the circumference should be individualized. Degree of PAB should be guided not only by SpO_2, HR, BP, CVP, and SvO_2 but also be tailored by right ventricular pressure by placement of trans-ventricular canula. We also integrated the information on ventricular contraction, AV-valve function, interventricular septum position, and tricuspid annular plane systolic excursion (TAPSE) from the TEE. Taken together, multimodal data integration is required to establish the optimal circumference of PAB (8,10).

In the present case, we monitored the change in TR severity to indirectly estimate right ventricular pressure, the contraction of both ventricles, and shift of the interventricular septum with TEE. PAB increases the afterload of the right ventricle and decreases the ejection from the right ventricle, which leads to the reduced blood return to the left ventricle. In addition, the geometric reduction of left ventricular cavity induces shift of the ventricular septum toward the left ventricle, that leads to the improvement of MR.

In our case, PAB enabled the ventricular septum to shift slightly to the left ventricle. MR was measured as mild at 19 weeks on preoperative TTE. The degree of MR improved after the PAB, to trivial, on TTE at four weeks after the procedure. Note that both exams were performed without general anesthesia.

The peak flow velocity of TR changed from 2.7 to 3.0 m/s immediately after PAB. In accordance to the Casthely *et al.*'s notion that optimal PAB increases systemic BP (11), systolic BP also increased after the PAB in current case. It is true that systolic BP is used as one indicator to judge the effect of PAB, however, systolic BP can vary depending on age, anesthesia, and in this case, dehydration. To compensate, we were also transfusing crystalloids and blood while banding the PA, thus, the increases of circulating blood volume may have been contributed concurrently with PAB to elevate the systemic blood pressure.

In the setting of cardiac surgery, rSO_2 indirectly provides data on left ventricular systolic and diastolic function (12), and rSO_2 has been reported to represent cerebral blood flow (13). Taken together, decreased cardiac systolic and diastolic function may increase vascular congestion, elevate pulmonary capillary wedge pressure, and mean pulmonary arterial pressure, that eventually rise CVP. Elevation of CVP further reduces cerebral perfusion pressure, represented by MAP–CVP, and cerebral blood flow, resulting in a decreased rSO_2.

Moreover, in the present case, we used rSO_2 as an indicator of oxygen delivery to the tissues (14), as cardiac output is a determinant of oxygen delivery. Although the absolute values of rSO_2 are not equal to the exact tissue oxygen saturation, it has been shown to correlate with SvO_2 (3), thus, rSO_2 may serve as an alternative monitoring method when SvO_2 monitoring is not possible.

We monitored rSO_2 and other hemodynamic parameters while surgeons banded the pulmonary artery to achieve both highest rSO_2 levels and stable hemodynamics. rSO_2 was 68% before banding, and increased and remained at over 90% after the banding at the same FiO_2 (*Figure 4*).

The INVOS 5100C (Covidien) sensors use light-emitting diodes to emit near-infrared light of two continuous wavelengths that penetrates bone (730 and 810 nm) from the sensor. The nature and quantity of the recaptured near-infrared light reflects the amount of deoxy-hemoglobin (HHb) and oxy-hemoglobin (O_2Hb), used to calculate regional cerebral oxygen saturation ($rScO_2$). The wavelengths reach to the 2 source-detector of 3 and 4 cm far, and they are used to obtain signals from deep brain tissue by superficial signals from skin and bone using the signals (i.e., spatially resoled spectroscopy). Detectors are located next to the light-emitting diodes. By subtracting the shallow (shorter) signal from the deeper (further) signal, surface interference contamination is minimized (15). Near-infrared cerebral oxygen monitoring is influenced by the partial pressure of arterial carbon dioxide, anemia, cranial distortion, cerebrospinal fluid layer, extracranial blood flow, and body position (16-20). However, these factors are likely to be minimized during cardiac surgeries where body positions, respiratory conditions and hemodynamics can be constantly maintained, and anemia may be adequately corrected as necessary. rSO_2 is a monitor that is sensitive to changes in hemodynamics, and its value is updated every 5 seconds.

If the hemodynamics changes due to the influence of the PAB, the output from the left ventricle will also be altered,

and cerebral blood flow will also be affected. Therefore, we proposed that PAB improves hemodynamics as a result of increased rSO_2. However, circulating blood volume was relatively decreased due to the preoperative diuretics and anesthesia-induced vasodilation. We administered fluids and performed blood transfusions. BP and CVP may have increased due to the fluids and blood transfusions, and an increase in rSO_2 due to improvement in anemia.

We may predict the increase or decrease in oxygen supply to the cerebrum by affixing a sensor to the anterior forehead. The advantages of rSO_2 are that the probe is handy and non-invasive. On the other hand, the disadvantages of rSO_2 are that the values being relative rather than absolute, and the cost. Decreased levels of rSO_2 (*vs.* baseline) indicate poor neurologic outcome in adults, and improved rSO_2 levels reduce postoperative delirium and cognitive decline. In contrast, in the pediatric population, there is insufficient data to conclude rSO_2 monitoring improves postoperative neurological outcomes. Taken together, cerebral rSO_2 monitoring may serve as one additional measure of the oxygen delivery to the brain, but it is not a sole universal guide for PAB placement particularly in vulnerable pediatric patients with dilated cardiomyopathy (DCM). Further outcome studies in pediatric population undergoing cardiac surgeries are warranted.

In summary, we report a successful pulmonary artery banding procedure performed for end-stage heart failure, with cerebral oximetry monitoring in a pediatric patient aged 5-month. Regional oxygen saturation may be of one further value to monitor cerebral oxygen delivery for the optimalization of pulmonary artery circumference while patients are undergoing pulmonary artery banding.

Acknowledgments

We would like to thank Dr. Ryojun Takeda (Nagano Children's Hospital, Medical Genetics), Dr. Tomomi Yamaguchi and Dr. Tomoki Kosho (Shinshu University Hospital, Medical Genetics) for their pivotal comments. We thank Ms. Yoshimi Sugino and Ms. Toshimi Kaneko for their technical assistance.
Funding: None.

Footnote

Reporting Checklist: The authors have completed the CARE reporting checklist. Available at https://dx.doi.org/10.21037/tp-21-340

Conflicts of Interest: All authors have completed the ICMJE uniform disclosure form (available at https://dx.doi.org/10.21037/tp-21-340). The authors have no conflicts of interest to declare.

Ethical Statement: The authors are accountable for all aspects of the work in ensuring that questions related to the accuracy or integrity of any part of the work are appropriately investigated and resolved. All procedures performed in studies involving human participants were in accordance with the ethical standards of the institutional and/or national research committee(s) and with the Helsinki Declaration (as revised in 2013). Written informed consent was obtained from the patient's parent/legal guardian for publication of this case report and accompanying images. A copy of the written consent is available for review by the editorial office of this journal.

References

1. Schranz D, Akintuerk H, Bailey L. Pulmonary Artery Banding for Functional Regeneration of End-Stage Dilated Cardiomyopathy in Young Children: World Network Report. Circulation 2018;137:1410-2.
2. Schranz D, Akintuerk H, Voelkel NF. 'End-stage' heart failure therapy: potential lessons from congenital heart disease: from pulmonary artery banding and interatrial communication to parallel circulation. Heart 2017;103:262-7.
3. Ricci Z, Garisto C, Favia I, et al. Cerebral NIRS as a marker of superior vena cava oxygen saturation in neonates with congenital heart disease. Paediatr Anaesth 2010;20:1040-5.
4. Sha K, Shimokawa M, Ishimaru K, et al. Differences in hemodynamic effects of amrinone, milrinone and olprinon after cardiopulmonary bypass in valvular cardiac surgery. Masui 2000;49:981-6.
5. Albus RA, Trusler GA, Izukawa T, et al. Pulmonary artery

banding. J Thorac Cardiovasc Surg 1984;88:645-53.
6. Towbin JA, Lorts A, Jefferies JL. Left ventricular non-compaction cardiomyopathy. Lancet 2015;386:813-25.
7. Kayvanpour E, Sedaghat-Hamedani F, Amr A, et al. Genotype-phenotype associations in dilated cardiomyopathy: meta-analysis on more than 8000 individuals. Clin Res Cardiol 2017;106:127-39.
8. Schranz D, Recla S, Malcic I, et al. Pulmonary artery banding in dilative cardiomyopathy of young children: review and protocol based on the current knowledge. Transl Pediatr 2019;8:151-60.
9. Agasthi P, Graziano JN. Pulmonary Artery Banding. In: StatPearls. Treasure Island (FL), 2021.
10. Schranz D, Rupp S, Müller M, et al. Pulmonary artery banding in infants and young children with left ventricular dilated cardiomyopathy: a novel therapeutic strategy before heart transplantation. J Heart Lung Transplant 2013;32:475-81.
11. Casthely PA, Redko V, Dluzneski J, et al. Pulse oximetry during pulmonary artery banding. J Cardiothorac Anesth 1987;1:297-9.
12. Paquet C, Deschamps A, Denault AY, et al. Baseline regional cerebral oxygen saturation correlates with left ventricular systolic and diastolic function. J Cardiothorac Vasc Anesth 2008;22:840-6.
13. Redlin M, Koster A, Huebler M, et al. Regional differences in tissue oxygenation during cardiopulmonary bypass for correction of congenital heart disease in neonates and small infants: relevance of near-infrared spectroscopy. J Thorac Cardiovasc Surg 2008;136:962-7.
14. Steppan J, Hogue CW Jr. Cerebral and tissue oximetry. Best Pract Res Clin Anaesthesiol 2014;28:429-39.
15. Dix LM, van Bel F, Baerts W, et al. Comparing near-infrared spectroscopy devices and their sensors for monitoring regional cerebral oxygen saturation in the neonate. Pediatr Res 2013;74:557-63.
16. Wong C, Churilov L, Cowie D, et al. Randomised controlled trial to investigate the relationship between mild hypercapnia and cerebral oxygen saturation in patients undergoing major surgery. BMJ Open 2020;10:e029159.
17. Yoshitani K, Kawaguchi M, Okuno T, et al. Measurements of optical pathlength using phase-resolved spectroscopy in patients undergoing cardiopulmonary bypass. Anesth Analg 2007;104:341-6.
18. Yoshitani K, Kawaguchi M, Miura N, et al. Effects of hemoglobin concentration, skull thickness, and the area of the cerebrospinal fluid layer on near-infrared spectroscopy measurements. Anesthesiology 2007;106:458-62.
19. Ogoh S, Sato K, Okazaki K, et al. A decrease in spatially resolved near-infrared spectroscopy-determined frontal lobe tissue oxygenation by phenylephrine reflects reduced skin blood flow. Anesth Analg 2014;118:823-9.
20. Closhen D, Berres M, Werner C, et al. Influence of beach chair position on cerebral oxygen saturation: a comparison of INVOS and FORE-SIGHT cerebral oximeter. J Neurosurg Anesthesiol 2013;25:414-9.

Cite this article as: Asano M, Doi K, Nomura M, Nagasaka Y. Cerebral oximetry-guided pulmonary artery banding for end-stage heart failure in a child with left ventricular noncompaction cardiomyopathy: a case report. Transl Pediatr 2021;10(11):3082-3090. doi: 10.21037/tp-21-340